Mehran University Research Journal of Engineering and Technology

https://doi.org/10.22581/muet1982.2203.20

2022, 41(3) 199-203

Spectroscopic properties of lithium like ions: Prospective elements for quantum computation

Salman Raza [a,*], Mehfooz Ali Abro [b], Saba Javaid [c], Roohi Zafar [c]

[a] *Department of Physics, University of Karachi, Karachi, Pakistan*

[b] *Oil and Gas Development Company Limited (OGDCL), Islamabad Pakistan*

[c] *Department of Physics, NED University of Engineering and Technology, Karachi*

[*] Corresponding author: Salman Raza, Email: salmanraza1928@gmail.com

Received: 07 January 2021, Accepted: 13 September 2021, Published: 01 July 2022

KEYWORDS

Rydberg atoms

Hydrogenic atoms

Quantum defects

Expectation values

Lithium like ions

Weakest bound electron

ABSTRACT

Rydberg physics is the most exquisite playground for the exploration of quantum technologies. Therefore, in this spectral investigation based on weakest bound electron potential model theory (WBEPMT). The quantum defects and Rydberg energies of low-lying and high-lying spectral Rydberg energy sequence in the following configurations: 1s2ns2Se1/2 and 1s2np2Po1/2 in Lithium-like ions (Z=4-6) Beryllium (Be II), Boron (B III) and Carbon (C IV) are computed with their radial expected values. Total 43 low-lying energies and quantum defects are computed and compared with 25 low lying radial expected values. The results are in good agreement with the previously published experimental / theoretical results. Based on the good agreement of low-lying data, total 257 new values of high-lying Rydberg energies and quantum defects are computed with 575 radial expected values currently not listed at NIST. The deviation in both sets of data doesn't exceed 1 cm^{-1}.

1. Introduction

The recent advancements in quantum technologies are based on a new highly tuneable, reproducible and 'mother's nature' most versatile building block for quantum systems called Rydberg atoms. That can be utilized as the platform for quantum computation. Especially, in the present scenario most important developing applications based on Rydberg atoms are quantum bits, quantum sensing and quantum imaging, and quantum optics. In the last decade the use of Rydberg atoms for quantum devices is developing at much faster pace than ever. However, at the moment we are very sure that as the field grows and develop, more and more quantum devices based on Rydberg atoms are available for commercial systems that will soon revolutionise the society and becomes helpful to solve a wide range of societal problems. correspondingly, a rapid evolution occurs in experimental techniques, such as Stark effect spectroscopy [1], millimetre wave technique [2], two or three-photon Doppler-free spectroscopy techniques [3] optical double-resonance and level-crossing techniques [4] etc. Regarding theoretical techniques various methods developed [5-7]. The exquisite theoretical techniques are self-consistent-field theory (SCFT) [8], many-body perturbation theory (MBPT) [9] and quantum defect theory (QDT) [10]. For the computation of spectral properties of many valence electrons atoms, these theoretical techniques show high complexity in computation. The solution provided by

Zheng *et.al* [11] by put forward a semi-empirical method called weakest bound electron potential model theory (WBEPMT). This theory based on a main idea of separating the ionic-core with the one most loosely bound electron called weakest bound electron (WBE). The ionic-core containing all remaining electrons called non-weakest bound electrons (NWBE's) and nucleus, in any atomic or ionic system. In weakest bound electron potential model (WBEPM) theory the ideas of quantum defects, foreign level configuration mixing, spectral Rydberg energy series and dependency of Rydberg states series on azimuthal quantum number was also presented. Based on the hypothetical ideas present in WBEPM theory various analytical investigations were performed for different elements neutral and ionic states successfully [12-31].

Within the limits of WBEPMT, Lithium like ions (Be II, B III and C IV) behave as hydrogen atom and single electron in their outer most orbit treated as WBE and the only difference is ionic-core containing nucleus and two NWBE's having a net charge of +1. In this way Lithium like ions (Be II, B III and C IV) WBE resides and moves in the potential of ionic-core.

The interpretation of the energy levels of the valence electron in Li like-ionic systems is peculiarly simple in a way that the WBE resides in the nuclear charge coulombic field, shielded by the two electrons of the K-shell. Electron's interaction effect can be neglected, and the main adjustment to the asymptotic coulomb potential is created by core-polarization effect. Thus, the problem can be solved by utilizing two different approaches; firstly, a model potential that is formulate to compute the observed quantum defects for the states of the WBE, and secondly, coupled equations that includes electron of S^e ground state and a P^o pseudo-state. These S^e and P^o utilized to write the Schrodinger equation of one electron system [32]. The results obtained within the frame work of WBEPM theory are essentially good and they have deviations of less than $1cm^{-1}$ for the allowed transitions discussed in previous literature published [12-31].

Another underlying purpose of this investigation lies in a particular observation during the beam foil spectroscopy (BFS). This observation offers another field of research in atomic spectroscopy called 'doubly excited states' [33]. Specially observe in the BFS of Lithium-like and Beryllium-like atoms [34].

For the doubly excited states, in three-electron systems, single excitation allows $2S^e$-doublet states with a single excited electron outside the $1s^21S^e$ closed shell core, whereas double excitation allows $4S^e$-quartet states where the three-electron spins are all aligned. On the experimental side, transitions between the doubly excited-states have been observed in the Li atom [35], and the beam-foil spectroscopy [36] has shown strong excitation of the preceding transitions. On the basis of these experimental observations since 1959, extensive theoretical investigations of the lithium isoelectronic series have been the objective of physicists. Among the methods applied to the ground state properties of Li-like ions are the wave functions method used by Patil [37], the Hylleraas-type variational method, and the 1/Z expansion perturbation theory used by Yan et al. [38], the Hylleraas coordinates employed by Perkins [39], Ho [40], and King [41], the full core plus correlation method utilized by Chung and Zhu [42], and the quasi-projection operator technique developed by Temkin et al. [43]. But, the treatment of the properties in three-electron systems remains a very complex physical problem. As a result, it is necessary to overcome such physical problems in the framework of simple analytical models. For this purpose, we have presented a new analytical model named the WBEPMT [44]. This method permits one to succeed in obtaining simple expressions of the Rydberg energies and Radial expected values in connection with an understanding of the importance of WBE-NWBE's correlation effects in atoms. The advantages of the WBEPM theory have been demonstrated previously [12-31]. In this paper, this method is applied to the computation of the radial expectation values of Lithium-like ions (Be II, B III and C IV) with their quantum defects and low-lying and high-lying spectral Rydberg energy sequence in $1s^2ns^2S^e_{1/2}$ and $1s^2np^2P^o_{1/2}$ up to $n=50$ electron's state.

2. Theory

The theory based on the concept of one electron problem like hydrogen atoms. In such systems every atomic or ionic system contains a single most loosely bound electron in valence shell termed as WBE and an ionic-core having +(Z-1) charge. The ionic core formed by the combination of leftover electrons other than WBE termed as NWBE's with nucleus. Due to shielding effect ionic core formed a net columbic potential in which WBE may polarize or penetrate towards ionic core and forms a dipole. Many quanta mechanical properties of the atomic or ionic system are depend upon the behaviour of WBE. Therefore, the accurate and precise information about WBE is advantageous. So, by treating WBE as one electron problem. The Hamiltonian function can be written as Eq. 1.

$$H_i = -\frac{1}{2}\nabla_i^2 + V(r_i) \quad (1)$$

For describing the potential of an ionic core in which WBE reside, the one electron Schrodinger equation can be written as Eq. 2.

$$\left(-\frac{1}{2}\nabla_i^2 + V(r_i)\right)\psi_i = \epsilon_i \quad (2)$$

Herein, potential $V(r_i)$ can be written as Eq. 3.

$$V(r_i) = \frac{\alpha}{r_i} + \frac{\beta}{r_i^2} \quad (3)$$

Herein,

$$\alpha = -Z^* \quad (4)$$

$$\beta = \frac{a(a+1) + 2al}{2} \quad (5)$$

In the above Eq. 3 α is the effective nuclear charge Z^*, r_i is the distance between WBE and the nucleus and l are the azimuthal quantum number of the WBE. Introduction of a is the parameter into the expression of the potential of ionic core need to be computed.

Also, in the potential Eq. 3, the first term gives coulombic potential and the second term gives electric dipole potential due to the dipole formed between ionic core and WBE.

Now, by solving Eqs. 1 and 3 for the potential of an ionic core, we get Eq. 6.

$$\left\{-\frac{h^2}{8\pi^2 m}\nabla_i^2 + \frac{A}{r_i} + \frac{B}{r_i^2}\right\}\Psi_i = \varepsilon_i \Psi_i \quad (6)$$

The Eq. 6 can be expressed in polar coordinates as Eq. 7.

$$\frac{1}{r^2}\frac{\partial}{\partial r}\left(r^2\frac{\partial \Psi}{\partial r}\right) + \frac{1}{r^2\sin\theta}\frac{\partial}{\partial\theta}\left(\sin\theta\frac{\partial\Psi}{\partial\theta}\right) + \frac{1}{r^2\sin^2\theta}\frac{\partial^2\Psi}{\partial\varphi^2} + \frac{8\pi^2 m}{h^2}\left\{\varepsilon - \frac{A}{r} - \frac{B}{r^2}\right\}\Psi = 0 \quad (7)$$

Where, $\Psi(r,\theta,\varphi) = R(r)Y_l^m(\theta,\varphi)$, and

$$Y_l^m(\theta,\varphi) = Ae^{\pm im\varphi}\Theta_{l,m}(\theta). \quad (8)$$

Now, by utilizing polar coordinates and separating the angular function $Y_{l,m}(\theta,\phi)$ from the radial function $R(r)$, we obtain Eq. 9.

$$\frac{d^2R}{dr^2} + \frac{2}{r}\frac{dR}{dr} + 2\left(\epsilon - \frac{A}{r} - \frac{B}{r^2} - \frac{l(l+1)}{2r^2}\right)R = 0 \quad (9)$$

We set Eq. 10.

$$2B + l(l+1) = l^* \quad (10)$$

And, substituting Eqs. 4 and 10 in Eq. 9, we obtain

$$\frac{d^2R}{dr^2} + \frac{2}{r}\frac{dR}{dr} + 2\left(\epsilon - \frac{Z^*}{r} - \frac{l^*(l^*+1)}{2r^2}\right)R = 0 \quad (11)$$

By substituting Eq. 3 into Eq. 10 and solving the one electron Schrodinger equation by a small modification of Hydrogen atom problem we get the following expressions (Eqs. 12-15).

$$l^* = l + d \quad (12)$$

$$n^* = n + d \quad (13)$$

$$\epsilon = -\frac{Z^*}{2n^*} \quad (14)$$

$$R = Cexp\left(-\frac{Z^*r}{n^*}\right)r^{l^*}L_{n-l-1}^{2l^*+1}\left(\frac{2Z^*r}{n^*}\right) \quad (15)$$

Where, l^* is the effective azimuthal quantum number and n^* is the effective principal quantum number C is a normalization constant and $L_{n-l-1}^{2l^*+1}[\frac{2Z^*r}{n^*}]$ is the generalized Laguerre polynomial. Using the normalization condition, we get Eq. 16.

$$\int_0^\infty |R(r)|^2 r^2 dr = 1 \quad (16)$$

And, the integral formula concerned with two generalized Laguerre polynomials is given as Eq. 17.

$$\int_0^\infty t^\lambda e^{-t}L_m^\mu(t)L_{m'}^{\mu'}(t)dt = (-1)^{m+m'}\Gamma(\lambda+1)\sum_k \binom{\lambda-\mu}{m-k}\binom{\lambda-\mu'}{m'-k}\binom{\lambda+k}{k} \quad (17)$$

Where, $Re(\lambda) > -1$. We can solve for the normalization constant as Eq. 18.

$$C = \left(\frac{2Z^*}{n^*}\right)^{\frac{3}{2}}\left(\frac{2Z^*}{n^*}\right)^{l^*}\sqrt{\frac{(n-l-1)!}{2n^*\Gamma(n^*+l^*+1)}} \{\exp\left(-\frac{Z^*r}{n^*}\right)r^{l^*}L_{n-l-1}^{2l^*+1}\left(\frac{2Z^*r}{n^*}\right)] \quad (18)$$

The solution may be used to calculate expectation values. For a transition from the level (n_f, l_f) to the level (n_i, l_i), the expectation value of r^k is $< n_f l_f |r^k| n_i l_i >$.

$$< n_f l_f |r^k| n_i l_i > = (-1)^{n_f+n_i+l_f+l_i}\left(\frac{2Z_f^*}{n_f^*}\right)^{l_f^*}\left(\frac{2Z^*}{n_i^*}\right)^{l_i^*} \quad (19)$$

$$\left(\frac{Z_f^*}{n_f^*} + \frac{Z_i^*}{n_i^*}\right)^{-l^*-l_i^*-k-3}\left[\frac{n_f^{*4}\Gamma(n_f^*+l_f^*+1)}{4Z_f^{*3}(n_f-l_f-1)!}\right]^{-\frac{1}{2}}\left[\frac{n_i^{*4}\Gamma(n_i^*+l_i^*+1)}{4Z_i^{*3}(n_i-l_i-1)!}\right]^{-\frac{1}{2}} \quad (20)$$

$$\sum_{m_1=0}^{n_f-l_f-1}\sum_{m_2=0}^{n_i-l_i-1}\frac{(-1)^{m_2}}{m_1!\,m_2!}\left(\frac{Z_f^*}{n_f^*}-\frac{Z_i^*}{n_i^*}\right)^{a}\left(\frac{Z_f^*}{n_f^*}+\frac{Z_i^*}{n_i^*}\right)^{-a}$$

Where, $a = m_1 + m_2$ (21)

$$\Gamma\left(l_f^* + l_i^* + m_1 + m_2 + k + 3\right) \quad (22)$$

$$\sum_{m_3=1}^{S}\binom{l_i^* - l_f^* + k + m_2 + 1}{n_f^* - l_f^* - 1 - m_1 - m_3}\binom{l_f^* - l_i^* + k + m_1 + 1}{n_i^* - l_i^* - 1 - m_2 - m_3}\binom{l_i^* - l_f^* + k + m_1 + m_2 + m_3 + 2}{m_3} \quad (23)$$

Where, $S = \min\left(n_f - l_f - 1 - m_1, n_i - l_i - 1 - m_2\right)$ and $k > -l_f^* - l_i^* - 3$.

If we let $k = 1$ and $f = i$, we can further derive Eq. 24.

$$< r >= \frac{3n^{*2} - l^*(l^*+1)}{2Z^*} \quad (24)$$

Where, $< r >$ is the Radial expectation value of the weakest bound electron *i*.

The negative value of ϵ of the weakest bound electron in Eq. 14 equal to the ionization energy of the weakest bound electron that is Eq. 25.

$$I = -\epsilon = \frac{Z^{*2}}{2n^{*2}} \quad (25)$$

Where, n^* is the effective principal quantum number. The Z^* and n^* are unknown values and are calculated by the transformation between Eigen-values of quantum defect theory (QDT) and WBEPM theory, which gives Eq. 26.

$$\frac{Z^*}{n^*} = \frac{Z_o}{n-\delta_n} \quad (26)$$

Where, Z_o is the atomic kernel net charge number and δ_n is the Quantum defect as a function of principal quantum number *n*.

During the process of successive ionization there are many possible values of ionization limits, corresponding to different WBE in each residual ion, provided that each residual ion should lie in the ground state. Therefore, the energy of the source atom, in which all electrons and nucleus are infinitely apart from each other, we have Eq. 27.

$$E = -\sum_{i=0}^{N} I_i \quad (27)$$

Where, *E* is the total electronic energy of source system in its ground state, I_i are the ionization limits at each stage of ionization. Thus, there is no problem of freezing orbits in the ionization procedure [45-47].

Now, the WBE of an atom or residual-ion is considered to be rotated around an ionic-core. So, the term energy of spectrum like Rydberg energy levels (*E*) is equal to the sum of ionization limit (E_{limit}) and Rydberg energy (E') of WBE.

$$E = E_{lim} + E' \quad (28)$$

We can rewrite Eq. 28 as Eq. 29.

$$\mathrm{E} = \mathrm{E_{lim}} - \frac{1}{2}\left(\frac{\mathrm{Z_o}}{\mathrm{n}-\delta_\mathrm{n}}\right)^2 \quad (29)$$

The Quantum defect (δ_n) without considering perturbation correction is computed by Martin's equation (Eq. 30) [48].

$$\delta_n = \sum_{i=1}^{4} a_i\, m^{-2(i-1)} \quad (30)$$

Where, δ_0 is the lowest Rydberg state Quantum defect of the series, coefficients ($a_{i's}$, i =1,2,3,4) in Eq. 30 are obtained by the method of least-square fitting of the first few low-lying experimental values of the Rydberg energy states of the given series [48].

3. Results and Discussion

In this investigation spectral properties of Lithium like-ions (Be II, B III and C IV) is presented in which 6 series having configurations: $1s^2ns^2S^e_{1/2}$, $1s^2np^2P^o_{1/2}$ are computed by utilizing coupled equations developed in semi-empirical method developed by Zheng et al. [44]. Total 43 low-lying Rydberg energy levels are listed at NIST [50] for above mentioned spectral series in lithium like-ions. The program is developed base on the coupled equations (see Eqs. 24, 29 and 30) in the theory [44]. The program first compute and compared quantum defects and Rydberg energies of 43 low lying levels by computing the coefficients of coupled equations (listed in Table 1). The deviation with the previously published expected values listed at NIST is not greater than 1 cm^{-1} (listed in Tables 2-7). In the second part program utilized the quantum defects determined in the first part of investigation and compute and compared 25 low-lying expected radial values listed in previously published paper [49]. The deviation is not greater than 0.1 cm^{-1}, except for few values (listed in Tables 2-7). Since the computed data agrees well with the previously published experimental / theoretical data [49]. The program finally computes the quantum defects, Rydberg energy levels and radial expected values up to *n* = 50.

Table 1

The coefficients of coupled Eqs. 24, 29 and 30 with nature of series

Lithium Like-Ions	E_{lim} [50] cm^{-1}	Series	δ_0	a_1	a_2	a_3	a_4	δ_{50}	Nature of Series
Be II (Z = 4), Li isoelectronic sequence	146882.86	$1s^2ns^2S^e_{1/2}$	0.26429	0.25953	0.04385	-0.12908	0.50433	0.25955	low lying core-penetration
		$1s^2np^2P^o_{1/2}$	0.04591	0.04998	-0.01018	-0.03036	0.03747	0.04998	High lying core-polarization
B III (Z = 5), Li isoelectronic sequence	305930.8	$1s^2ns^2S^e_{1/2}$	0.19731	0.19321	0.03998	-0.14276	0.64072	0.19323	low lying core-penetration
		$1s^2np^2P^o_{1/2}$	0.04184	0.04419	-0.00494	-0.02360	0.03064	0.04418	High lying core-polarization
C IV (Z = 6), Li isoelectronic sequence	520175.3	$1s^2ns^2S^e_{1/2}$	0.15763	0.15393	0.03472	-0.07139	0.25934	0.15395	low lying core-penetration
		$1s^2np^2P^o_{1/2}$	0.03708	0.03831	0.00036	-0.03389	0.05515	0.03831	High lying core-penetration

Table 2

Spectral Rydberg Energy Series with Quantum Defects and Radii of Li iso-electronic sequence in $1s^2ns\ ^2S^e_{1/2}$ (Be II)

State	Quantum Defects		Rydberg Energies (cm^{-1})		$R_{y\ (NIST)}$-R_y (cm^{-1})	Radii (cm^{-1})	
n	$\delta_{(NIST)}$ [50]	δ	$R_{y\ (NIST)}$ [50]	R_y		$< r >$	$< r >$ [49]
3	0.264	0.264	88231.915	88231.91	0.000	5.662	5.613
4	0.262	0.262	115464.44	115464.44	0.000	10.527	10.479
5	0.261	0.261	127335.12	127335.12	0.000	16.890	16.843
6	0.261	0.261	133556.44	133556.44	0.000	24.752	24.711
7	0.260	0.260	137218.78	137218.73	-0.047	34.114	
8	0.260	0.260	139555.16	139555.06	-0.096	44.976	
9	0.260	0.260	141136.3	141136.15	-0.150	57.338	
10		0.260		142255.65		71.199	
20		0.260		145756.17		292.309	
30		0.260		146386.33		663.418	
40		0.260		146604.66		1184.525	
50		0.260		146705.18		1855.633	

Table 3

Spectral Rydberg Energy Series with Quantum Defects and Radii of Li iso-electronic sequence in $1s^2np^2P^o_{1/2}$ (Be II)

State	Quantum Defects		Rydberg Energies (cm^{-1})		$R_{y\,(NIST)}$-R_y (cm^{-1})	Radii (cm^{-1})	
n	$\delta_{(NIST)}$ [50]	δ	$R_{y\,(NIST)}$ [50]	R_y		< r >	< r > [49]
2	0.046	0.046	31928.744	31928.74	0.000	2.398	2.364
3	0.048	0.048	96495.36	96495.36	0.000	6.069	6.034
4	0.049	0.049	118760.51	118760.51	0.000	11.243	11.207
5	0.050	0.050	128971.62	128971.62	0.000	17.917	17.880
6	0.050	0.050	134485.37	134485.15	-0.216	26.091	26.058
7	0.050	0.050	137795.97	137795.73	-0.241	35.766	
8	0.050	0.050	139938.08	139937.80	-0.276	46.941	
9	0.050	0.050	141403.24	141402.94	-0.299	59.616	
10		0.050		142448.99		73.791	
20		0.050		145779.72		298.040	
30		0.050		146393.25		672.290	
40		0.050		146607.57		1196.540	
50		0.050		146706.67		1870.790	

Table 4

Spectral Rydberg Energy Series with Quantum Defects and Radii of Li iso-electronic sequence in $1s^2ns^2S^e_{1/2}$ (B III)

State	Quantum Defects		Rydberg Energies (cm^{-1})		$R_{y\,(NIST)}$-R_y (cm^{-1})	Radii (cm^{-1})	
n	$\delta_{(NIST)}$ [50]	δ	$R_{y\,(NIST)}$ [50]	R_y		< *r* >	< *r* > [49]
3	0.197	0.197	180201.92	180201.92	0.000	3.954	3.928
4	0.195	0.196	237698.27	237698.27	0.000	7.263	7.237
5	0.195	0.195	263159.78	263159.78	0.000	11.571	11.545
6	0.194	0.194	276630.32	276630.32	0.000	16.879	
7	0.194	0.194	284609.86	284610.00	0.139	23.187	
8	0.194	0.194	289723.38	289723.53	0.155	30.494	
9	0.194	0.194	293195.66	293195.80	0.138	38.801	
10		0.194		295660.87		48.109	
20		0.193		303413.34		196.178	
30		0.193		304819.18		444.247	
40		0.193		305307.54		792.315	
50		0.193		305532.68		1240.383	

Table 5

Spectral Rydberg Energy Series with Quantum Defects and Radii of Li iso-electronic sequence in $1s^2np^2P^o_{1/2}$ (B III)

State	Quantum Defects		Rydberg Energies (cm^{-1})		$R_{y\,(NIST)}$-R_y (cm^{-1})	Radii (cm^{-1})	
n	$\delta_{(NIST)}$ [50]	δ	$R_{y\,(NIST)}$ [50]	R_y		$< r >$	$< r >$ [49]
2	0.042	0.042	48358.335	48358.33	0.000	1.604	1.584
3	0.043	0.043	192951.23	192951.23	0.000	4.059	4.037
4	0.044	0.044	242829.74	242829.74	0.000	7.514	7.493
5	0.044	0.044	265721.62	265721.62	0.000	11.970	11.947
6	0.044	0.044	278090.15	278089.36	-0.791	17.425	
7	0.044	0.044	285519.29	285518.73	-0.557	23.881	
8	0.044	0.044	290327.86	290327.43	-0.432	31.337	
9		0.044		293617.33		39.792	
10		0.044		295966.68		49.248	
20		0.044		303450.77		198.806	
30		0.044		304830.19		448.364	
40		0.044		305312.16		797.922	
50		0.044		305535.05		1247.480	

Table 6

Spectral Rydberg Energy Series with Quantum Defects and Radii of Li iso-electronic sequence in $1s^2ns^2S^e_{1/2}$ (C IV)

State	Quantum Defects		Rydberg Energies (cm^{-1})		$R_{y\,(NIST)}$-R_y (cm^{-1})	Radii (cm^{-1})	
n	$\delta_{(NIST)}$ [50]	δ	$R_{y\,(NIST)}$ [50]	R_y		$< r >$	$< r >$ [49]
3	0.158	0.158	302849	302849.00	0.000	3.046253	3.029605
4	0.156	0.156	401348.1	401348.10	0.000	5.557480	5.540836
5	0.155	0.155	445368.5	445368.50	0.000	8.818055	8.801080
6	0.155	0.155	468784	468784.00	0.000	12.828333	12.806610
7	0.155	0.155	482706	482705.43	-0.570	17.588428	
8	0.154	0.154	491650.8	491649.97	-0.832	23.098400	
9	0.154	0.154	497736.7	497735.64	-1.060	29.358286	
10		0.154		502062.75		36.368109	
20		0.154		515717.41		147.714878	
30		0.154		518204.23		334.060815	
40		0.154		519069.43		595.406536	
50		0.154		519468.64		931.752172	

Table 7

Spectral Rydberg Energy Series with Quantum Defects and Radii of Li iso-electronic sequence in $1s^2np^2P^o_{1/2}$ (C IV)

State	Quantum Defects		Rydberg Energies (cm^{-1})		$R_{y(NIST)}$-R_y (cm^{-1})	Radii (cm^{-1})	
n	$\delta_{(NIST)}$ [50]	δ	$R_{y(NIST)}$ [50]	R_y		$< r >$	$< r >$ [49]
2	0.037	0.037	64484	64484.00	0.000	1.209	1.266
3	0.038	0.038	320050.1	320050.10	0.000	3.054	3.030
4	0.038	0.038	408311.1	408311.10	0.000	5.650	5.541
5	0.038	0.038	448855.8	448855.80	0.000	8.996	8.801
6	0.038	0.038	470775	470774.60	-0.401	13.092	12.807
7	0.038	0.038	483948.4	483947.33	-1.069	17.939	
8	0.038	0.038	492477.7	492476.35	-1.354	23.535	
9		0.038		498313.08		29.881	
10		0.038		502482.03		36.977	
20		0.038		515768.94		149.190	
30		0.038		518219.42		336.403	
40		0.038		519075.82		598.615	
50		0.038		519471.90		935.828	

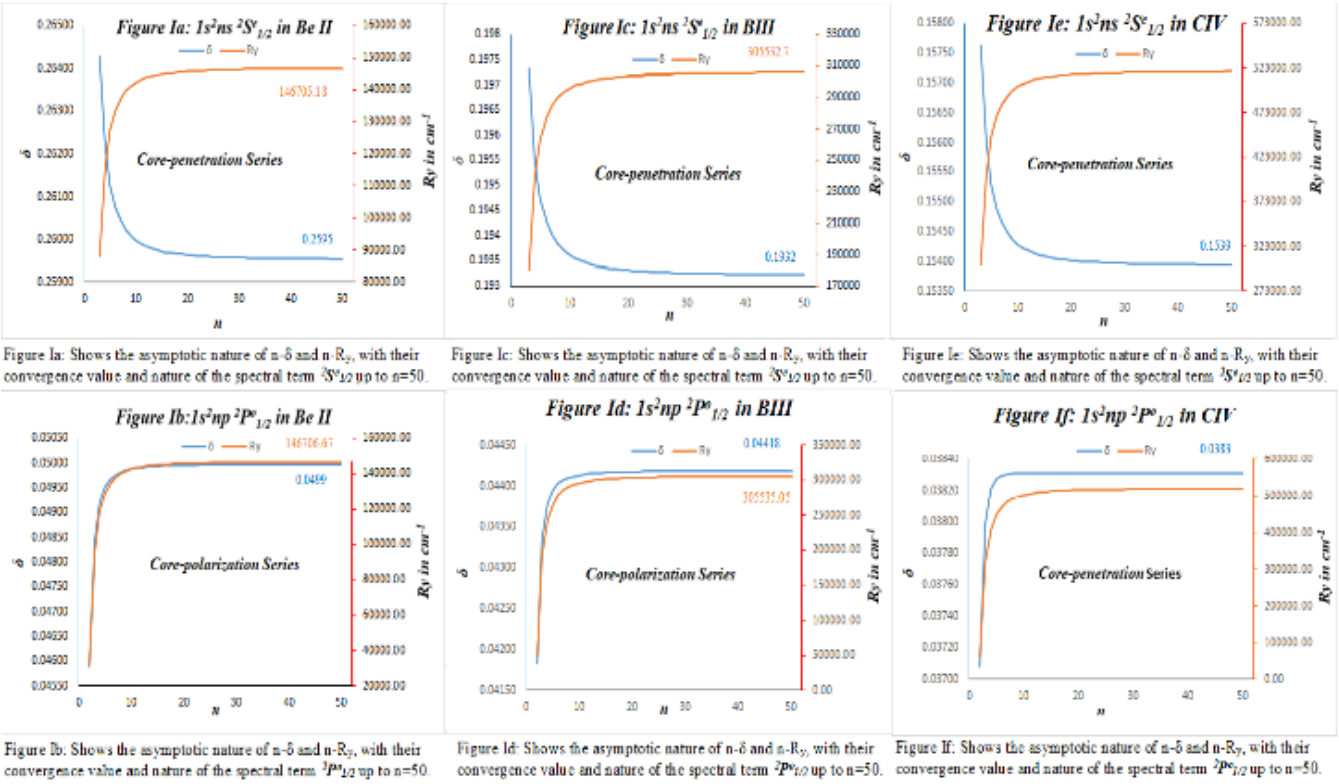

Figure Ia: Shows the asymptotic nature of n-δ and n-R_y, with their convergence value and nature of the spectral term $^2S^e_{1/2}$ up to n=50.

Figure Ic: Shows the asymptotic nature of n-δ and n-R_y, with their convergence value and nature of the spectral term $^2S^e_{1/2}$ up to n=50.

Figure Ie: Shows the asymptotic nature of n-δ and n-R_y, with their convergence value and nature of the spectral term $^2S^e_{1/2}$ up to n=50.

Figure Ib: Shows the asymptotic nature of n-δ and n-R_y, with their convergence value and nature of the spectral term $^2P^o_{1/2}$ up to n=50.

Figure Id: Shows the asymptotic nature of n-δ and n-R_y, with their convergence value and nature of the spectral term $^2P^o_{1/2}$ up to n=50.

Figure If: Shows the asymptotic nature of n-δ and n-R_y, with their convergence value and nature of the spectral term $^2P^o_{1/2}$ up to n=50.

Fig. 1. *n*-δ and n-Ry curves in comparisons for Z = 4-6, up to n = 50 for $1s^2ns^2S^e_{1/2}$ and $1s^2np^2P^o_{1/2}$. Showing the core penetration nature for all $1s^2ns^2S^e_{1/2}$ and the core polarization in $1s^2np^2P^o_{1/2}$ for Z = 4 and 5, but an exception is occurred at Z = 6, that is core penetration in $1s^2np^2P^o$1/2

For all above mentioned 6 series in Lithium like-ions having configurations $1s^2ns^2S^e_{1/2}$, $1s^2np^2P^o_{1/2}$, the coefficients of coupled equations (Eqs. 24, 29 and 30), a_i's$_{(i = 1,2,3,4)}$ and δ_0, are computed by low-lying expected value listed at NIST [50]. In Table 1, one can easily observe that the nature and convergence of series

depends upon the 1st two coefficients (a_1, a_2) of Eq. 30. In the case all unperturbed series, all series of quantum defects converge towards the a_1, i.e. $a_1 = \delta_{50}$ and by the sign of a_2 the nature of series can be easily determined; i.e., if a_2 is positive the series is core-penetration series and if a_2 is negative the series is core penetration series.

The results compute in the present computation for spectral Rydberg energy series of Lithium like-ions up to n = 50 and Z = 4-6 are listed in Tables 2-6. Due to the constancy of quantum defects and degeneracy of Rydberg states at higher n only few computed values are shown in Tables 2-6. The detail evaluation is shown in Fig. 1. The comparison with previously published data [49-50] shows good agreement with the computed values. The absolute deviation in general is not greater than 1 cm^{-1}.

Also, in the graphical section by plotting graphs of quantum defects and Rydberg levels as a function of principal quantum numbers called n-δ and n-R_y curves. The change in the regularity of the quantum defects and Rydberg energy levels series can be easily observed with the convergence under same ionization limit and nature of series as describe in Table 1.

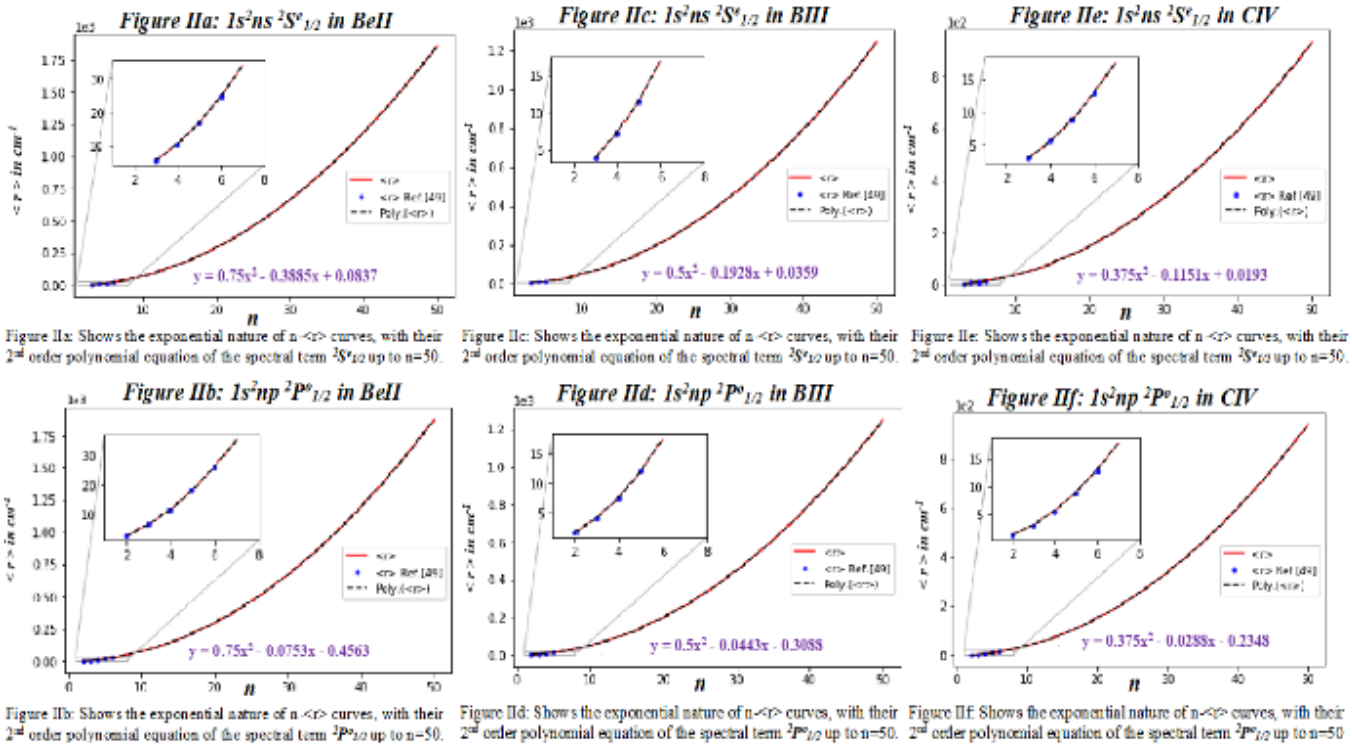

Figure IIa: Shows the exponential nature of n-<r> curves, with their 2nd order polynomial equation of the spectral term $^2S^e_{1/2}$ up to n=50.
Figure IIc: Shows the exponential nature of n-<r> curves, with their 2nd order polynomial equation of the spectral term $^2S^e_{1/2}$ up to n=50.
Figure IIe: Shows the exponential nature of n-<r> curves, with their 2nd order polynomial equation of the spectral term $^2S^e_{1/2}$ up to n=50.
Figure IIb: Shows the exponential nature of n-<r> curves, with their 2nd order polynomial equation of the spectral term $^2P^o_{1/2}$ up to n=50.
Figure IId: Shows the exponential nature of n-<r> curves, with their 2nd order polynomial equation of the spectral term $^2P^o_{1/2}$ up to n=50.
Figure IIf: Shows the exponential nature of n-<r> curves, with their 2nd order polynomial equation of the spectral term $^2P^o_{1/2}$ up to n=50

Fig. 2. n-<r> curves show good agreement between computed and previously published excepted value for $1s^2ns^2S^e_{1/2}$ and $1s^2np^2P^o_{1/2}$ configurations in lithium like-ions for Z = 4-6, up to n = 50. Also presented general 2nd order polynomial equation for each series

All $1s^2ns^2S^e_{1/2}$ series in lithium like ions are low-lying core penetration series, converges under same ionization potentials. In 3 n-δ curves, at low n curve first decreases exponentially shows the regular decrease in Quantum defects and at high n the constancy of Quantum defects shows by asymptotic nature. In contrast, in 3 n-R_y curves at low n the curve first increases exponentially shows the regular increase in the Rydberg States energy and at high n the degeneracy of Rydberg energy states shows by asymptotic nature. Similarly, in $1s^2np^2P^o_{1/2}$ series in Lithium like-ions 2 out of 3 are high-lying core polarization series, except 1 in C IV shows high-lying core-penetration series converges under same ionization potentials. In 3 n-δ curves, at low n curve first increases exponentially shows the regular increase in Quantum defects and at high n the constancy of Quantum defects shows by asymptotic nature. In all n-R_y curves shows the same behaviour as in low-lying core penetration series (see Fig. 1).

Finally, in the graphs of radial expected values as the function of principal quantum numbers called n-<r> curves (see Fig. 2). The computed curves fitted quite

well with the curves of previously published data [49]. By curve fitting the general equation of 2nd order polynomial for each series of Radial expected values are also presented with each graph (see Fig. 2). Within the same series as the *n* increase the Radial expected value increases exponentially in each case. But as the *Z* increases the Radial expected values decrease in comparison from *Z* = 4-6 in both configurations: $1s^2ns^2S^e_{1/2}$, $1s^2np^2P^o_{1/2}$. So, it can be concluded that at high *Z* the probability of finding WBE near an ionic-core increase where it can polarize or penetrate towards an ionic-core forming a strong dipole generating both kind of spectral series, core penetration as well as core-polarization series under same ionization limit.

4. Conclusion

Within the limits of semi-empirical method, relatively have simple analytical solutions utilizing the coupled equations. The results computed for the quantum defects, Rydberg energy levels and expected radial values for ns and np states for *Z* = 4-6, up to *n* = 50 are accurate and shows good accordance with previously published values [49-50].

The graphical description clearly presents the nature and convergence of all series. In general, all *ns* series belongs to core-penetration and all *np* series belongs to core-penetration series with an exception in C IV both *ns* and *np* series belongs to low and high-lying core-penetration series (see Fig. 1 and Table 1).

The Radial expected values having great importance in computation of transition probabilities are not only agreed well with the previously published data [49]. A general 2nd order polynomial equation for each series is also generated by curve fitting shows an excellent agreement with both computed and previously published data [49].

5. Acknowledgement

All authors would like to thanks Dr. Zaheer-Uddin, Department of Physics, University of Karachi for his kind assistance during the research.

6. References

[1] G. U. Bublitz, S. G. Boxer, “Stark spectroscopy: applications in chemistry, biology, and materials science”, Annual Review of Physical Chemistry, vol. 48, no. 1, pp. 213-242, 1997.

[2] C. Fabre, S. Haroche, P. Goy, “Millimeter spectroscopy in sodium Rydberg states: Quantum-defect, fine-structure, and polarizability measurements”, Physical Review A, vol. 18, no. 1, p. 229, 1978.

[3] T. W. Hänsch, S. A. Lee, R. Wallenstein, C. Wieman, “Doppler-Free Two-Photon Spectroscopy of Hydrogen 1S− 2S”, Physical Review Letters, vol. 34, no. 6, p. 307, 1975.

[4] J. Larsson, “Optical Double Resonance and Level-Crossing Spectroscopy Using Pulsed Laser Excitation”, Lund Reports in Atomic Physics, 1987.

[5] I. P. Grant, B. J. McKenzie, P. H. Norrington, D. F. Mayers, N. C. Pyper, “An atomic multiconfigurational Dirac-Fock package”, Computer Physics Communications, vol. 21, pp. 207-231, 1980.

[6] J. Máššik, I. Hubačc, P. Mach, “Applicability of quasi-degenerate many-body perturbation theory to quasi-degenerate electronic states: The H4 model revisited”, International Journal of Quantum Chemistry, vol. 53, no. 2, pp. 207-228, 1995.

[7] C. F. Fischer, J. E. Hansen, “Theoretical oscillator strengths for the resonance transitions in the Zn I isoelectronic sequence”, Physical Review A, vol. 17, no. 6, pp. 19-56, 1978.

[8] J. Hinze, C. C. Roothaan, “Multi-configuration self-consistent-field theory”, Progress of Theoretical Physics Supplement, vol. 1, no. 40, pp. 37-51, 1967.

[9] R. J. Bartlett, G. D. Purvis, “Many-body perturbation theory, coupled-pair many-electron theory, and the importance of quadruple excitations for the correlation problem”, International Journal of Quantum Chemistry, vol. 14, no. 5, pp. 561-581, 1978.

[10] M. J. Seaton, “Quantum defect theory”, Reports on Progress in Physics, vol. 46, no. 2, p. 167, 1983.

[11] N. W. Zheng, T. Wang, D. X. Ma, T. Zhou, J. Fan, “Weakest bound electron potential model theory”, International Journal of Quantum Chemistry, vol. 98, no. 3, pp. 281-290, 2004.

[12] H. Shizhong, and S. Qiufeng, “Calculation of the Rydberg Energy Levels for Francium Atom”, Physics Research International, vol. 2010, pp. 1-5, 2010.

[13] G. Çelik, S. Ateş, S. Özarslan, and M. Taşer, “Transition probabilities, oscillator strengths and lifetimes for singly ionized magnesium”, Journal of Quantitative Spectroscopy and Radiative Transfer, vol. 112, no. 14, pp. 2330-2334, 2011.

[14] C. Zhou, J. J. Cao, L. Liang, and L. Zhang, “Theoretical calculation of energy levels of Pb III”, Turkish Journal of Physics, vol. 35, no. 1, pp. 37-42, 2011.

[15] S. Ateş, G. Çelik, G. Tekeli, and M. Taşer, “Oscillator strengths of allowed transitions for O III”, Atomic Data and Nuclear Data Tables, vol. 98, no. 1, pp. 1-18, 2012.

[16] G. Çelik, D. Doğan, S. Ateş, and M. Taşer, “Transition probabilities and radiative lifetimes of levels in FI”, Atomic Data and Nuclear Data Tables, vol. 98, no. 4, pp. 566-588, 2012.

[17] G. Çelik, D. Doğan, S. Ateş, and M. Taşer, “Electric quadrupole transition probabilities for singly ionized magnesium”, Journal of Quantitative Spectroscopy and Radiative Transfer, vol. 113, no. 12, pp. 1601-1605, 2012.

[18] M. Yildiz, “Energy levels and atomic lifetimes of Rydberg states in neutral Indium”, Acta Physica Polonica A, vol. 123, no. 1, pp. 25-30, 2013.

[19] M. Yildiz, Y. Gökçe, and G. Çelik, “Electric dipole radiative lifetimes for neutral boron atom”, Indian Journal of Physics, vol. 87, no. 11, pp. 1069-1073, 2013.

[20] G. Çelik, E. Erol, and M. Taşer, “Transition probabilities, oscillator strengths and radiative lifetimes for Zn II”, Journal of Quantitative Spectroscopy and Radiative Transfer, vol. 129, pp. 263-271, 2013.

[21] S. Ateş, and H. H. Uğurtan, “Lifetimes of excited levels for atomic silicon”, Indian Journal of Physics, vol. 87, no. 1, pp. 9-17, 2013.

[22] S. Ateş, Y. Gökçe, G. Çelik, and M. Yıldız, “Oscillator strengths and transition probabilities for singly ionized terbium”, Canadian Journal of Physics, vol. 92, no. 9, pp. 1043-1046, 2014.

[23] G. Çelik, S. Ateş, and G. Tekeli, “Electric dipole transition probabilities, oscillator strengths, and lifetimes for Co16+”, Canadian Journal of Physics, vol. 94, no. 1, pp. 23-25, 2015.

[24] G. Çelik, and S. Ateş, “E1 and E2 transitions for Fe XVI, Co XVII and Ni XVIII”, Astrophysics and Space Science, vol. 361, no. 7, pp. 2-29, 2016.

[25] A. Maireche, “New Higher Excited Energy Levels of Rydberg States for Weakest Bound Potential Model Theory: Extended Quantum Mechanics”, Journal of Nano-and Electronic Physics, vol. 9, no. 4, pp. pp. 1-7, 2017.

[26] E. Ahmed, and J. Akbar, “Rydberg Energy Levels and Quantum Defects of some Semiconductor Elements”, Journal of Basic and Applied Sciences, vol. 14, pp. 113-118, 2018.

[27] N. Ali, M. N. Hameed, S. Raza, and A. A. Azam, “Theoretical Investigation of Radiative Lifetimes and Rydberg Levels Sequence in Indium I”, Journal of Natural Sciences and Research, vol. 8, no. 17, pp. 29-50, 2018.

[28] S. Raza Khan, M. N. Hameed, and N. Ali, “Spectral Energies and Radiative Lifetimes of Rydberg States in Neutral Hydrogen”, Journal of Natural Sciences and Research, vol. 8, no. 14, pp. 37-45, 2018.

[29] S. Raza, M. A. Shahzad, S. Naeem, “Precise Computation of Energy Levels and Radiative Lifetimes in the s, p, d, and f Sequence of Hydrogen Isotope, with Natural Linewidths”, Journal of Natural Sciences and Research, vol. 9, no. 10, pp. 47-64, 2019.

[30] R. Siddique, S. Raza, N. Ali, and Z. Uddin, “On Some Perturbed Series of Neutral Strontium”, Science International, vol. 5, no. 31, pp. 699-705, 2019.

[31] E. Ahmed, S. Raza, M. N. Hameed, M. Farooq, and J. Akbar, “Rydberg energy levels and Quantum defects of B II, Ge II, Si II of subgroups III and IV”, Canadian Journal of Physics, vol. 98, no. 3, pp 274-286, 2020.

[32] G. Peach, H. E. Saraph, and M. J. Seaton, “Atomic data for opacity calculations. IX. The lithium isoelectronic sequence”, Journal of Physics B: Atomic, Molecular and Optical Physics, vol. 21, no. 22, pp. 36-69, 1988.

[33] C. L. Cocke, “Beam-Foil Spectroscopy”, Methods in Experimental Physics, vol. 13, pp. 213-272, 1976.

[34] I. Martinson, “Beam-foil spectroscopy”, In Treatise on Heavy-Ion Science, Springer, pp. 423-489, 1985.

[35] G. Herzberg, and H. R. Moore, “The spectrum of Li+”, Canadian Journal of Physics, vol. 37, no. 11, pp. 1293-1313, 1959.

[36] H. G. Berry, “Multiply-excited states in beam-foil spectroscopy”, Physica Scripta, vol. 12, no. 5, pp. 1-2, 1975.

[37] S. H. Patil, “Wave functions for two-and three-electron atoms and isoelectronic ions”, The European Physical Journal D-Atomic, Molecular, Optical and Plasma Physics, vol. 6, no. 2, pp. 171-177, 1999.

[38] Z. C. Yan, M. Tambasco, and G. W. F. Drake, “Energies and oscillator strengths for lithiumlike ions”, Physical Review A, vol. 57, no. 3, pp. 16-52, 1998.

[39] J. F. Perkins, “Hylleraas-type calculations of the ground states of the Li isoelectronic sequence through Z = 8”, Physical Review A, vol. 13, no. 3, pp. 9-15, 1976.

[40] H. Y. Lin, et al., “Excellent color quality of white-light-emitting diodes by embedding quantum dots in polymers material”, IEEE Journal of Selected Topics in Quantum Electronics, vol. 22, no. 1, pp. 35-41, 2015.

[41] F. W. King, “Calculations on the S2 ground states of some members of the Li I isoelectronic series”, Physical Review A, vol. 40, no. 4, pp. 17-35, 1989.

[42] J. J. Hsu, K. T. Chung, and K. N. Huang, “P^o4 series of lithium”, Physical Review A, vol. 49, no. 6, pp. 44-66, 1994.

[43] A. Temkin, A. K. Bhatia, and J. N. Bardsley, “Resonance Quasi-Projection Operators: Calculation of the S2 Autoionization State of He”, Physical Review A, vol. 5, no. 4, pp. 16-63, 1972.

[44] N. W. Zheng, T. Wang, D. X. Ma, T. Zhou, and J. Fan, “Weakest bound electron potential model theory”, International Journal of Quantum Chemistry, vol. 98, no. 3, pp. 281-290, 2004.

[45] C. Monroe, “Quantum information processing with atoms and photons”, Nature, vol. 416, no. 6877, pp. 238-246, 2002.

[46] T. G. Walker, and M. Saffman, “Consequences of Zeeman degeneracy for the van der Waals blockade between Rydberg atoms”, Physical Review A, vol. 77, no. 3, pp. 1-18, 2008.

[47] M. D. Lukin, M. Fleischhauer, R. Cote, L. M. Duan, D. Jaksch, J. I. Cirac, and P. Zoller, “Dipole blockade and quantum information processing in mesoscopic atomic ensembles”, Physical Review Letters, vol. 87, no. 3, pp. 1-4, 2001.

[48] W. C. Martin, “Series formulas for the spectrum of atomic sodium (Na I)”. Journal of the Optical Society of America, vol. 70, no. 7, pp. 784-788, 1980.

[49] N. W. Zheng, et al., “Transition probability of lithium atom and lithiumlike ions with weakest bound electron wave functions and coupled equations”, International Journal of Quantum Chemistry, vol. 76. no. 1, pp. 51-61, 2000.

[50] A. Kramida, Yu. Ralchenko, J. Reader, and NIST ASD Team, “NIST Atomic Spectra Database (ver. 5.8)”, National Institute of Standards and Technology, Gaithersburg MD. 2020.

7. Explanation of Tables

Table 1

Shows the coefficients of coupled Eqs. 24, 29 and 30 with nature of series for Lithium like-ions.

Lithium Like-Ions: Shows the nomenclature, atomic number and electronic sequence of ionic state.

a_1: 1st Coefficient of Eq. 30 for both ns and np series.

a_2: 2nd Coefficient of Eq. 30 for both ns and *np* series.

a_3: 3rd Coefficient of Eq. 30 for both *ns* and *np* series.

a_4: 4th Coefficient of Eq. 30 for both *ns* and *np* series.

δ_0: Quantum defects of lowest possible state of each series.

δ_{50}: Quantum defects of highest state of each series.

Tables 2-7

Quantum Defects and Rydberg Energies and Radii of Spectral Rydberg series up to n =50 in Be II, B III and C IV.

State: Principal Quantum number.

$\delta_{(NIST)}$ [50]: Computed values of Quantum defects by utilizing energy levels listed at NIST [50].

δ: Computed values of Quantum defects by Eq. 30.

$R_{y(NIST)}$ [50]: Experimental values of Spectral Rydberg energies listed at NIST [50] in cm^{-1}.

R_y: Spectral Rydberg energies computed By WBEPMT in cm^{-1}.

$R_{y(NIST)}$-R_y: Deviation between excepted values listed at NIST with the values computed in this work in cm^{-1}.

$\langle r \rangle$: Radial expected values computed in this work by WBEPMT.

$\langle r \rangle$ [49]: Radial expected values from previously published data [49].